Hemodynamic Analysis of Coronary Artery Microcirculation Using a Pig's Morphometric Data

Sehyun Shin*, Jungsu Park
School of Mechanical Engineering, Kyungpook National University, 1370 Sangyeok-Dong, Buk-ku, Daegu 702-701, Korea

Stenosed coronary artery may play an important role in various coronary heart diseases. However, it has not been known how much stenosed coronary artery affects coronary circulation system, quantitatively. The present study developed a mathematical model for microcirculation in the left common coronary artery (LCCA) with adopting a previously measured morphological data and mechanical properties of the coronary vessels. We examine the effect of percent diameter stenosis on blood flow rate and shear stress for two cases. Case I comprised of one-stenosed element at 10^{th} order (% diameter stenosis are 10, 30, and 50, respectively). Case II consisted of completely occluded element at 10^{th} order (number of occluded elements are 0, 1, and 2 out of 8, respectively). As the level of stenosis becomes severe, the shear stress increases significantly but the flow rate reduction was relatively small. However, for the occluded case, there was linearly proportional reduction of flow rate according to number of occluded elements. Either such high shear stress associated with coronary artery stenosis or reduced flow rate due to occlusion may cause atherosclerosis and myocardial ischemia.

Key Words : Left common Coronary Artery (LCCA), Hemodynamics, Stenosis, Occlusion

Nomenclature

D : Diameter (μm)
L : Length (mm)
N : Number of coronary artery vessel
P : Pressure (mmHg)
$\dot{Q}$: Flow rate (ml/sec)
μ : Viscosity (mPa·s)

Subscript

n : Order number

1. Introduction

It has been known that coronary circulation plays an important role in various coronary heart diseases. The function of the coronary network is to supply the heart with oxygen and nutrients and remove its waste, which is critical to the overall workings of the heart. Additionally, the hemodynamics of the coronary circulation shows a number of interesting phenomena. For example, blood in coronary artery flows during diastolic period whereas systemic blood flows during systolic period. Another thing is that coronary vascular system consists of number of bifurcation in small amount of space to distribute blood to the myocardial system. In fact, coronary artery disease (CAD) used to exhibit a stenosis of artery, which is a reduction of cross-sectional area of artery. Such stenosis of coronary artery may play an important role on the pathogenesis of chronic vascular disease and progression of vascular occlusion. However, it has not been known how stenosis of coronary artery is associated with development of CAD.

In general, the coronary artery bifurcates into the right coronary artery (RCA) and the left common coronary artery (LCCA) as shown in

* Corresponding Author,
E-mail : shins@knu.ac.kr
TEL : +82-53-950-6570; **FAX** : +82-53-956-7907
School of Mechanical Engineering, Kyungpook National University, 1370 Sangyeok-Dong, Buk-ku, Daegu 702-701, Korea. (Manuscript **Received** March 3, 2004; **Revised** March 29, 2005)

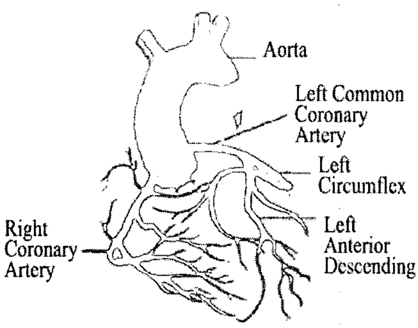

Fig. 1 Schematic of coronary circulatory system

Fig. 1. The LCCA bifurcates into the left anterior descending (LAD) artery and left circumflex (LCx) artery. Both LAD and LCx branch into many small vessels and capillary vessels. Kassab et al. (1993) provided a full set of vascular morphometric data of a pig's RCA and LCCA by measuring the dimensions in diastole. There have been many experimental and modeling studies in order to understand the factors that influence coronary circulation. There are a few theoretical approaches in studying coronary circulation. One is a mathematical model with anatomical morphometric data of the coronary vessels. The other uses an electric circuit analog or lumped parameter model.

In the mathematical model of the vessel network, there are two common models : Weibel's bifurcation model (Wiener, 1963) and Strahler's rivulets model (Strahler, 1952). Kassab et al. (1990) modified the latter model by taking into consideration the vessel diameter variation. The modified model is called the "diameter-defined Strahler model," i.e., the Strahler model with the addition of a rule based on the diameter of the blood vessels. Additionally, Kassab et al. (1997) improved the analysis of coronary circulation by introducing the following concepts : 1) the segment and element used to express the series-parallel feature of blood vessels ; 2) the longitudinal position matrix to describe the longitudinal position of the daughter vessels along the length of their parent vessels. Kassab and his coworkers investigated the pressure distribution, flow rate, and the effect of vessel compliance on the flow rate.

After reviewing the previous studies, we have not found an answer to the question how stenosis of coronary artery may play an important role on the pathogenesis of chronic vascular disease and progression of vascular occlusion. Therefore, the objectives of the present study are to analyze the hemodynamic characteristics of the coronary circulation and to examine the effect of percent diameter stenosis on blood flow rate and shear stress for two cases.

2. Method

2.1 Mophormetric data

The organs of each species are called homologous when they have a different function or geometry but come ontogenically from the same origin. The hearts of pig and humans belong to homologous organs. A pig's coronary arteries and veins are topologically tree-like. The coronary capillaries are network-like. In order to model the tree-like coronary arteries, the capillary blood vessels are defined as vessels of an order 0. The smallest arterioles are assigned an order 1. When the two arterioles of order 1 meet, the confluent vessel is given an order 2 if its diameter exceeds the mean diameter of the order 1 vessels by an amount specified by the formula (Kassba et al., 1993), or remain as order 1 if the diameter of the confluent is not larger than the amount. This process is continued until all arterial segments are arranged in increasing diameter and are assigned the order numbers 1, 2, 3, $\cdots$, n.

Fig. 2 shows a schematic of the morphometric analysis of the LCCA with the terminology. As shown in Figure 2, each blood vessel between the two nodes of bifurcation is called a "segment". These serially connected segments function as a single tube in hemodynamics, each tube of which is called an "element". The geometry of the arterial tree is specified by the statistical data of lengths and diameters of all order vessels and the connectivity matrix C_{mn}. The connectivity matrix C_{mn} is defined as the ratio of the total number of elements of order m that spring directly from the parent elements of order n, divided by the total number of the elements of order n.

The present vascular model considered all the statistical data, including the mean of the diameters and lengths of vessels, and the mean connectivity matrix. In fact, the connectivity matrix is replaced by the branching ratio, a diagonal matrix of the connectivity matrix. The branching ratio is defined as the ratio of the number of elements of the order m divided by the number of elements of the order $n+1$. In the present model, we assumed that all vessel elements at any order are parallel each other and the blood pressure at the same order junctions are equal. The result of the present model was compared with those of the previous model (Kasab et al., 1997), which considered all the statistical data, including the mean and standard deviation of the diameters and lengths of vessels, and the mean connectivity matrix.

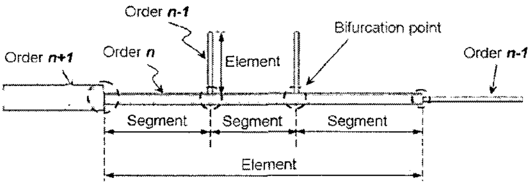

Fig. 2 Schematic of the terminology for the morphometric data of LCCA

Coronary artery disease in the LCCA used to occur around the LAD. This is the same place as the vessel of order 10 which is branched out from the LCCA. In the present study, the hydrodynamic changes for the two pathological cases of the coronary blood vessels were investigated as shown in Table 1. Numerical analyses were performed on those with one element of order 10 with stenosis, one or two elements of order 10 with occlusion.

2.2 Mathematical model

The present study adopted the coronary mor-

Table 1 Diameter, length, and number of vessel elements in each order of vessels in the porcine LCCA

Order	Diameter (μm)	Length (mm)	Number of order	Branching Ratio	Reynolds number	Womersley number
0a	6.2	0.052	1,789,365	3.38		
1	9.0	0.115	530,045	2.63	0.100	0.004
2	12.1	0.136	201,823	3.17	0.157	0.005
3	17.1	0.149	63,723	2.44	0.294	0.007
4	30.1	0.276	26,120	2.99	0.349	0.011
5	65.2	0.508	8,739	4.23	0.444	0.023
6	138	1.42	2,066	4.08	0.766	0.048
7	290	3.68	506	2.99	1.636	0.100
8	460	5.58	169	3.52	3.101	0.159
9	778	11.8	48	6.00	6.376	0.269
10	1695	23.9	8	8.00	17.671	0.586
11	3276	52.9	1		73.144	1.132

Table 2 Case Studies

Case I	One element of order 10 with 10, 30 or 50 percent diameter stenosis	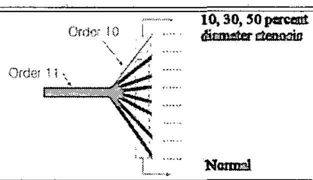
Case II	One or two elements of order 10 with occlusion	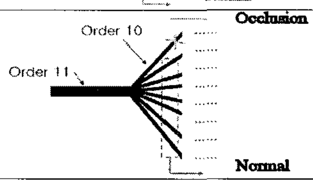

phometry provided by Kassab et al. (1993) and a mathematical model for the LCCA of a pig was utilized. Table 2 represents the morphometric data of a pig's LCCA including the vessel diameter, length, number of vessel elements in each order, and the branching ratio.

In the present model, the nodes of the circuit were numbered serially. The volume flow rate through the two nodes i and j follows Poiseuille's equation :

$$\dot{q}_{ij}=\frac{\pi D_{ij}^4}{128\mu_{ij}L_{ij}}(P_i-P_j) \quad (1)$$

The total flow rate through these two nodes, $\dot{Q}_{ij}$, is the sum of each flow rate in the N parallel elements :

$$\dot{Q}_{ij}=N_{ij}\dot{q}_{ij}=N_{ij}\frac{\pi D_{ij}^4}{128\mu_{ij}L_{ij}}(P_i-P_j) \quad (2)$$

$$\dot{Q}_{ij}=G_{eq,ij}\Delta P_{ij} \quad (3)$$

where

$$G_{eq,ij}=\frac{\pi N_{ij}D_{ij}^4}{128\mu_{ij}L_{ij}} \text{ and } \Delta P_{ij}=P_i-P_j \quad (4)$$

Applying the law of conservation of mass at an arbitrary junction between an element having i^{th} order and the m number of elements having the j^{th} order, a set of linear algebraic equations for all of the nodes in the network can be obtained.

$$\sum_{i=1}^{m_j}\dot{Q}_{ij}=0 \quad (5)$$

$$\sum_{i=1}^{m_j}(P_i-P_j)\,G_{eq,ij}=0 \quad (6)$$

In the present study, 11 equations having the 1^{st} order were generated and solved by using Gauss elimination method (Datta, 1995) to transform the matrix into triangular one. As a result, the exit pressure at each order can be obtained and the corresponding flow rate can be calculated by using the Poiseuille's equation.

On setting up the hemodynamic equations, blood flow is dependent upon Reynolds number (Re) and Wormersley number (Wo) as follows :

$$\mathrm{Re}_n=\frac{\rho V_n D_n}{\mu_n} \quad (7)$$

$$Wo_n=\frac{D_n}{2}\sqrt{\frac{\rho\omega}{\mu_n}} \quad (8)$$

where ω and ρ represent the radian frequency and density whose values were 110 cycle/min and 1.05 g/cm^3. In the coronary arteries, the Womersley numbers are smaller than 1 and Reynolds numbers are smaller than 1 in the coronaries of an order 5 or smaller and are several hundred in the largest coronary arteries. In most coronary arteries, the flow can be approximated by Poiseuille flow except for the larger coronary arteries. Thus, Poiseuille's equation is utilized in analyzing the coronary artery flow. It was found that the Reynolds number and Womersley number in the present study were smaller enough to be satisfied with Poiseuille's equation as listed in Table 1.

After obtaining the flow rate, the shear stress and the shear rate at each order number can be determined from the following definitions :

$$\dot{\gamma}_n=\frac{32q_n}{\pi D^4}=8\frac{V_n}{D_n} \quad (9)$$

$$\tau_n=\mu_n\cdot\dot{\gamma}_n \quad (10)$$

The boundary conditions were given as follows :

P=100 mm Hg	at the Sinus of Valsalva
P=26 mm Hg	at the capillary network

In general, shear-thinning characteristics are shown in blood which consist of plasma and blood cells. Since blood velocity in a small capillary vessel is so small, the corresponding viscosity is expected to be large but the actual viscosity is small. There are several mechanisms involved in a small blood vessel such as the "Fahraeus-Lindqvist effect" and cell migration. It is commonly known that blood viscosity decreases with a decrease in blood vessel diameter, which is called the "Fahraeus-Lindqvist effect" (Fahraeus et al., 1931). Additionally, in a small vessel, blood cells tend to migrate into the center of the axis, which results in a cell-free-layer near the vessel wall. Furthermore, there occurs a decrease of hematocrits in a small vessel, which is called the Fahraeus effect. The present study adopted the viscosity coefficient in the coronary circulation taking into consideration the Fahraeus-Lindqvist model (Albrecht et al., 1979) as shown in Fig. 3. In this figure, the rectangular symbols

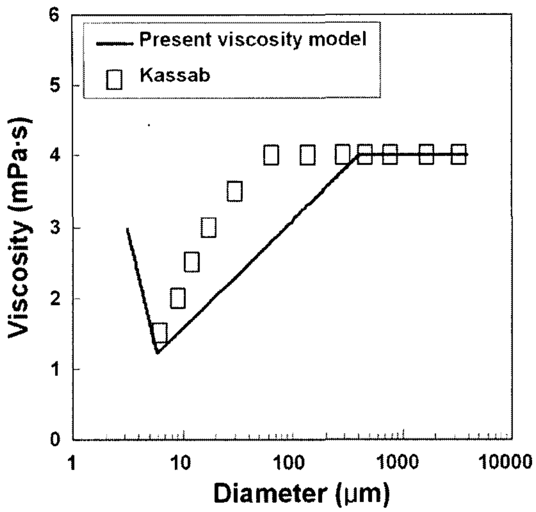

Fig. 3 Viscosity model for microcirculation

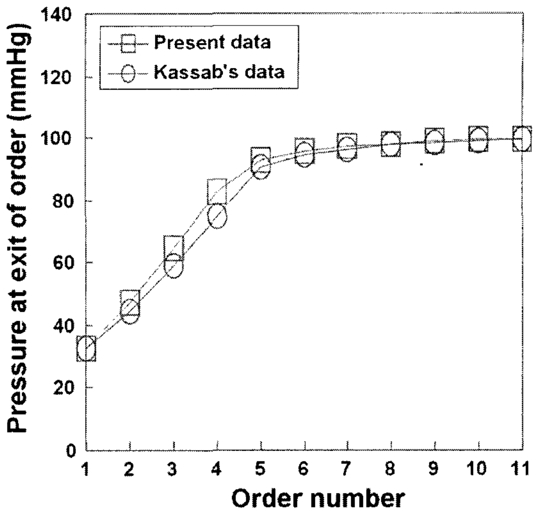

Fig. 4 Relationship between the blood pressure at exit of an element of n order and the order number for LCCA

represent the viscosity model used by Kassab, whereas the line indicates the model used in the present study. In Fig. 3, the present viscosity model can better describe the Fahraeus-Lindqvist effect in a small vessel below 6 μm than Kassab's model (1993).

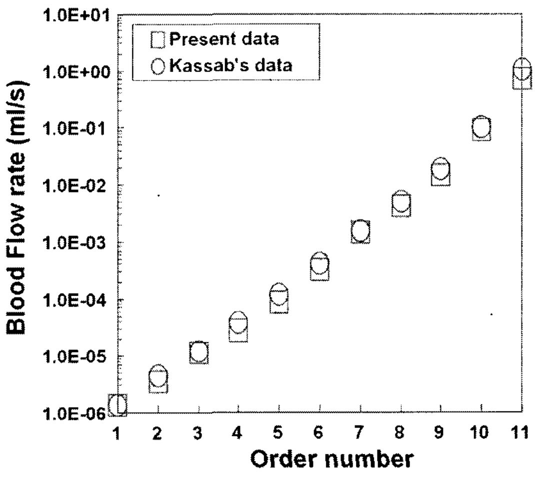

Fig. 5 Relationship between the blood flow rate and the order number for the LCCA

3. Results and Discussion

Prior to examining the effect of stenosis on hemodynamic characteristics, we compared the present numerical results with the previous one. Fig. 4 shows the mean values of the distribution of longitudinal pressure which are the analytic solutions to Eq. (1) in the present model. A comparison of the blood pressure in the coronary blood vessels shows that the present results are in good agreement with Kassab's results (1993) over ranges of order numbers except for in the small arteries of orders 3 to 4. Moreover, Figure 5 shows the coronary blood flow per element of the present calculation in the symmetric LCCA model and Kassab's results (1993). It is found that the present mathematical model yields a similar blood flow per element to that of the Kassab's model.

We examined the effect of percent diameter stenosis on blood flow rate and shear stress for two cases. Case I comprised of one-stenosed element at 10^{th} order (% diameter stenosis are 10, 30, and 50, respectively). Fig. 6 shows the changes in the flow rates for three different stenoses in an element out of eight parallel elements at order 10. Even for the 50% diameter stenosis case, there does not show any noticeable difference from the reference. This is attributed to the fact that the resistance of an element of order 10 is significantly small compared with the total resistance of order 10.

However, as shown in Fig. 7, the stenosis at Order 10 strongly affected the shear stress. As the severity of stenosis becomes deeper, the shear stress increases significantly. For 50% diameter stenosis, the shear stress was increased eight times larger than that in the normal element. The abnormal high shear stress in blood vessel might cause a dysfunction of endothelial cells and subsequent atherosclerosis of coronary artery. In fact, Fry (1973) reported that there was an impairment in the hemoendotheliocyte due to the high shear stress. Nerem (1992) reported that shear stress is an important factor which causes atherosclerosis. As discussed above, there is only a 4% reduction in the flow rate due to the 50% diameter stenosis in the four elements. Thus, the major cause of stress increase is the reduction of the vessel diameter while the flow rate is almost the same.

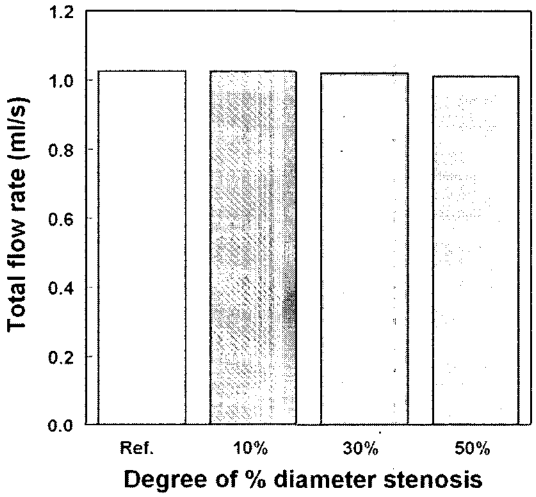

Fig. 6 Relationship between the degree of percent diameter stenosis and the total flow rate

Reviewing the results obtained from Figs. 6 and 7, we found that the flow rate is almost independent of the stenosis up to 50% diameter stenosis, whereas the shear stress for stenosed artery having an almost same flow rate is strongly dependent of the percent diameter stenosis. In order to keep constant flow rate in the stenosed artery, the velocity should be increased as square function of diameter from a simple basic equation ($Q=\pi r^2 V$).

Additionally, we examine the effect of occlusion on blood flow rate (Case II). Case II consisted of completely occluded element at 10^{th} order and the number of occluded elements are 0, 1, and 2 out of 8, respectively. Fig. 8 shows a reduction of the flow rate due to the occlusion of the elements of order 10. As the results show in Fig. 9, there are 12.5% and a 25% reduction in the flow rates due to occlusion of an element and two elements, respectively. If enough blood is not provided to the myocardial tissue, metabolites

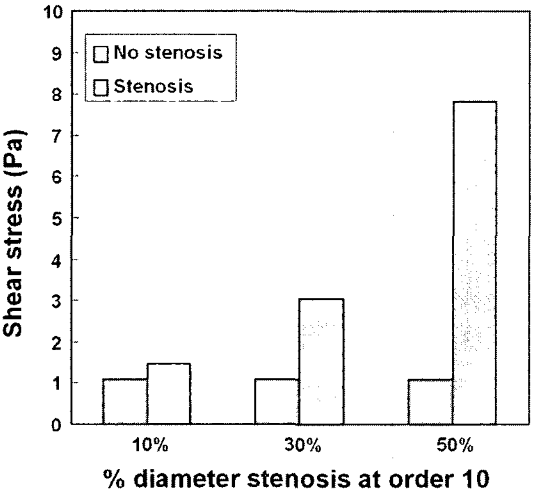

Fig. 7 Shear stress according to the percent diameter stenosis at an element of order 10

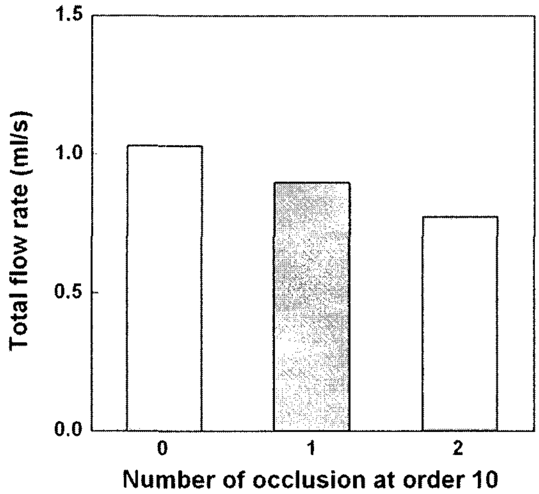

Fig. 8 Relationship between the number of occlusions at order 10 and the total flow rate

will collect in the tissue. This causes hypoxia which is a cause of ischemic heart diseases such as angina pectoris and myocardial infarction (Jennings et al., 1978). Reduction in the coronary blood flow (myocardial ischemia) may critically impair the mechanical behavior of the left ventricle.

However, when coronary occlusion occurs, collateral vessels are formed to supply blood to heart muscle tissue. In fact, there has not been enough experimental data for the collateral vessel structure. This may be the major obstacle to pursue numerical investigation with considering pathological conditions. These pathological considerations are beyond the scope of the present study, but should be considered in further study.

In the present study, we solved a number of matrix of Poiseullie equations based on assumption that the coronary blood flow is steady and the vessel diameter is constant that was measured during diastole. However, in fact, the coronary flow is pulsatile and the vessel diameter keeps changing with time. The developed mathematical models including present one are limited to consider such a dynamic conditions as they are. Thus, we ahave been conducting further study using a MatLab software, which can consider the pulsatile flow conditions and corresponding vessel dimensions during systolic and diastolic period.

4. Conclusions

Application of the LCCA mathematical model was developed based on the measured coronary morphometry in diastole and number of matrix of Poiseullie's equations. The present study was able to examine the effect of pathological cases on hydrodynamic characteristics considering the whole coronary arterial system, which can be used to delineate the initiating mechanism of the examined pathological cases from hemodynamic aspects. The present study found that the major cause of stress increase in coronary artery is the reduction of the vessel diameter while the flow rate is almost the same. The increase in the shear stress yields impairment in the hemoendotheliocyte and atherosclerosis, which lead to occlusion. Further study may be used to delineate the initiating mechanism of coronary artery diseases (CAD) related with hemodynamic variation with the present mathematical models.

Acknowledgments

This work is sponsored by Grants (R05-2003-000-11752) from the KOSEF.

References

Albrecht, K., Gaetgens, H., Pries, P. A. and Heuser, M., 1979, "The Fahraeus Effect in Narrow Capillaries (i.d. 3.3 to 11.0 μm)," *Microvasc. Res.*, Vol. 18, pp. 33~47.

Biswa Nath Datta, 1995, *Numerical Linear Algebra and Applications*, An International Thomson Publishing Company.

Fahraeus, R. and Lindqvist, T., 1931, "The Viscosity of the blood in narrow capillary tubes," *Am. J. Physiol.*, Vol. 96, pp. 562~568.

Fishback, M. E., Brunett, L. and Scher, A. M., 1959," Autoregulation of Coronary Blood Flow in the Dog Heart," *Clin. Res.*, Vol. 7, pp. 60~69.

Fry, D. L., 1973, Responses of the Arterial Wall to Certain Physical Factors. In : Porter R, Knight J, Editors. Atherogenesis : Initiating Factors, Amsterdam : Associated Scientific Publishers, pp. 93~125.

Jennings, R. B., Hawkins, H. K., Lowe, J. E., Hill, M. L., Klotman, S. and Reimer, K. A., 1978, "Relation Between High Energy Phosphate and Lethal Injury in Myocardial Ischemia in the Dog," *Am. J. Pathol.*, Vol. 92, pp. 187~214.

Kassab, G. S., 1990, Morphometry of the Coronary Arteries in the Pig, La Jolla : University of Califonia, San Diego, Ph. D. Dissertation.

Kassab, G. S., Berkley, J. and Fung, Y. C., 1997, "Analysis of Pig's Coronary Arterial Blood Flow with Detailed Anatomical Data," *Annals of Biomedical Engineering*, Vol. 25, pp. 204~217.

Kassab, G. S., Rider, C. A., Tang, N. J. and Fung, Y. C., 1993, "Morphometry of Pig Coronary Arterial Trees," *Am. J. Physiol. Heart Circ.*

Physiol., Vol. 265(34), pp. H350~H365.

Nerem, R. M., 1992, "Vascular Fluid Mechanics, the Arterial Wall and Atherosclerosis," *ASME J. Biomechanical Eng*., Vol. 114, pp. 274~282.

Strahler, A. N., 1952, Hypsometric (area altitude) analysis of erosional topology. Bull. Geol Sot. Amer. Vol. 63, pp. 1117~1142.

Wiener, F. R., 1963, *Morphometry of the Human Lung*, New York : Academic Press.